GLAUBER, R. & SCHOMAKER, V. (1953). *Phys. Rev.* **89**, 667-671.
HENDERSON, R. (1975). *J. Mol. Biol.* **93**, 123-138.
HENDERSON, R. & GLAESER, R. M. (1985). *Ultramicroscopy*, **16**, 139-150.
HO, M.-H., JAP, B. K. & GLAESER, R. M. (1988). *Acta Cryst.* A**44**, 878-884.
HOERNI, J. A. (1956*a*). *Phys. Rev.* **102**, 1530-1533.
HOERNI, J. A. (1956*b*). *Phys. Rev.* **102**, 1534-1542.
HOPPE, W. (1970). *Acta Cryst.* A**26**, 414-426.
ISAACSON, M., LANGMORE, J. P. & ROSE, H. (1974). *Optik (Stuttgart)*, **41**, 92-96.
JAP, B. K. & GLAESER, R. M. (1978). *Acta Cryst.* A**34**, 94-102.
JAP, B. K. & GLAESER, R. M. (1980). *Acta Cryst.* A**36**, 57-67.
POST, B. (1977). *Phys. Rev. Lett.* **39**, 760-763.
RAITH, H. (1968). *Acta Cryst.* A**24**, 85-93.
SHEN, W. & COLELLA, R. (1987). *Nature (London)*, **329**, 232-233.
UNWIN, P. N. T. & HENDERSON, R. (1975). *J. Mol. Biol.* **94**, 425-440.

Acta Cryst. (1989). A**45**, 628-635

Structural Comparisons Using Restrained Inhomogeneous Transformations

BY SIMON K. KEARSLEY

Merck Sharp & Dohme Research Laboratories, PO Box 2000, *Rahway, NJ* 07065, *USA*

(*Received* 5 *May* 1988; *accepted* 10 *April* 1989)

Abstract

Comparisons between structures with similar atomic skeletons are made by mathematically deforming one over the other using inhomogeneous transformations. Removal of shallow bending and twisting distortions between the structures reveals local differences that are masked by comparisons using homogeneous transformations. Inhomogenous deformations are restrained to prevent unrealistic changes in local atomic bonding geometry by the addition of penalty functions similar in form to the potentials used in empirical molecular mechanics calculations.

1. Introduction

On many occasions chemists dealing with atomic structures need to measure the similarity for arrangements of corresponding atoms between two structures. For instance, a common requirement of crystallographers is to determine the similarity between two or more molecules that may pack within the asymmetric unit; also, they may wish to decide whether there exists any pseudo spatial symmetry between such molecules. Often comparisons of experimental structures to ones predicted by theoretical models are used to detect anomalies that may exist in either one. For molecular mechanics calculations, especially those of macromolecules, one is never guaranteed to find the same equilibrium structure. If several subtly different structures are generated then methods to compare and contrast them are essential.

The most common way to make a comparison between two structures is to superimpose them such that the sum of the squared distances between corresponding atoms is a minimum. This method maintains rigid structural skeletons. The use of the root mean square (r.m.s.) deviation of distance between these atoms as the measure of similarity between structures is ubiquitous since it is easy to appreciate. Slightly more sophisticated comparisons also measure relative amounts of compression or expansion between structures. These types of comparisons, termed orthogonal and homogeneous transformations respectively, often make similar conformations look radically different or conceal local differences between structures. Fig. 1 shows this in a schematic manner. Comparison method *A* merely superimposes without structural distortion, and the deviations in the region of the glitch are of the same magnitude as other regions; in atomic structures such localized differences between the arrangement of atoms are not easily seen.

Inhomogeneous transformations allow various types of bending and twisting distortions to occur. Low-order inhomogeneous transformations are defined as ones that give moderately shallow deformations that apply uniformly over the entire structure. The use of these is not in vogue since the prospect of performing and interpreting the resulting structural distortions is forbidding. But more significantly the number of degrees of freedom, even for low-order deformations, increases rapidly (a 60-parameter fit

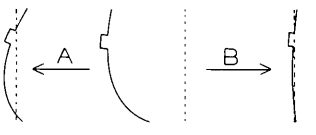

Fig. 1. Schematic illustration showing the effects of orthogonal (*A*) and inhomogeneous (*B*) comparison transformations.

0108-7673/89/090628-08$03.00

for a cubic as compared with a 6-parameter fit for an orthogonal transformation) and therefore restricts its use to large molecules where there are plenty of atoms to characterize the transformation sufficiently.

The aim of this paper is fourfold: (i) To show how inhomogeneous transformations can be utilized to remove low-order distortions that may conceal the salient differences between structures. Comparison method *B* in Fig. 1 removes the low-order curvature differences between the structures and the subsequent superposition clearly identifies the glitch as the only region of major difference. (ii) To show how inhomogeneous transformations may be restrained to prevent unrealistic distortions since there is little benefit in comparison transformations that *force fit* global features of structures at the expense of generating unreasonable localized distortions. (iii) To present techniques that extend the use of inhomogeneous transformations to smaller structures since comparison transformations that impose a precise overlap of corresponding atoms by wild variation in underdetermined deformation parameters will be of little use. (iv) Finally, more as a corollary, to suggest how inhomogeneous distortions can be constructed and used as templates to anneal or purposely bend and twist structures.

In the next few subsections we describe the features of the various types of transformations. § 2 shows how to implement a general inhomogeneous transformation including geometric restraints. Finally, a demonstration of the comparison techniques is given in § 3.

1.1. *Orthogonal transforms*

Orthogonal transformations require the determination of a translation vector **C** and a matrix R which describes the rotation which superimposes the structures into optimal least-squares atom–atom register. By definition the configuration of the atomic skeleton remains precisely the same before and after the orthogonal transformation. The transformation is written as

$$\mathbf{z}_L = \mathbf{C} + R\mathbf{x}_L \tag{1}$$

and the function minimized is the sum of the distances squared,

$$\varepsilon = \sum_L (\mathbf{z}_L - \mathbf{C} - R\mathbf{x}_L)^2 \tag{2}$$

where $\mathbf{z}_L$ are the reference structural coordinates, $\mathbf{x}_L$ are the object structural coordinates which are being transformed and subscript L refers to a particular atom. The determination of **C** is trivial for orthogonal and homogeneous transformations (§ 1.2) since the vector that superimposes the centroids is optimal (the centroid is the first moment of the structural coordinates). **C** can be removed by simply shifting the structures so that their respective centroids are at the origin. Finding R, the elements of which are not linearly independent, invariably involves some iterative optimization procedure using various formulations of the rotation matrix (Diamond, 1966; Cox, 1967; Rao & Rossman, 1973; Nyburg, 1974; Kenknight, 1984; Mackay, 1984; Lesk, 1986) or analytic approaches (Kabsch, 1976, 1978; McLachlan, 1972, 1979; Kearsley, 1989).

1.2. *Linear transforms*

A few investigators (Mackay, 1977; Watkin, 1980) have used a slightly more comprehensive transformation which describes homogeneous deformations of a structure.

$$\mathbf{z}_L = \mathbf{C} + D\mathbf{x}_L. \tag{3}$$

D is a 3×3 matrix that describes the variation of displacement of general positions **z** with respect to corresponding positions **x**; (3) serves to map specific points (atoms) $\mathbf{x}_L$ onto $\mathbf{z}_L$. The nine matrix elements are allowed to vary independently and can be derived using the linear least-squares method with a residual function of form similar to (2).

Matrix D can be factorized into an orthogonal matrix R which describes rotation and T which is a symmetric homogeneous dilation matrix accommodating six of the nine independent parameters. The tilde indicates the transpose of matrix D.

$$D = RT \tag{4}$$

$$T = (\tilde{D}D)^{1/2} \qquad R = D(\tilde{D}D)^{-1/2}. \tag{5}$$

R is not the optimal rotation matrix for an orthogonal transformation since it was derived in conjunction with the six degrees of freedom afforded by dilation. However, it presents a good starting matrix for finding the optimal orthogonal transformation if iterative procedures are used.

If T is diagonalized, the eigenvectors show the principal directions of strain and the eigenvalues give the relative degrees of dilation. The determinant of R ought to have a value of +1 for a proper rotation. If this is not so, it means that the transformation inverted the structure with concomitant changes in chirality. This factorization of D is also applicable to higher-order transformations and serves to inform us of possible structural inversions.

1.3. *Higher-order transforms*

Inhomogeneous transformations allow for variations of R, which represent curvature differences between the structures (these are seen as bending and twisting distortions), and variation of T, which reflect changes in strain throughout the structure. Continuum mechanics expresses such bending and twisting distortions as derivatives of D with respect to the

object structural coordinates. The first and second derivatives of D define the quadratic and cubic deformation tensors.

$$D_{ki} = \partial z_k / \partial x_i \qquad E_{kij} = \partial D_{ki} / \partial x_j = \partial^2 z_k / \partial x_j \, \partial x_i$$

Linear tensor — Quadratic tensor

$$F_{kijl} = \partial^2 D_{ki} / \partial x_i \, \partial x_j = \partial^3 z_k / \partial x_l \, \partial x_j \, \partial x_i. \qquad (6)$$

Cubic tensor

Diamond's (1976) definitive treatment of the quadratic transformation rigorously analyzed the E_{kij} tensor and interpreted the variation of rotation in terms of curvatures along and about the principal directions of strain and identified curvature-free deformations describing the variations of T through the structure. Transformation orders higher than quadratic are less open to this sort of interpretation; however, it will be seen that they are necessary for certain types of common distortions. In this article the highest transformation considered will be cubic, although extension to quartic or even higher orders presents little complication.

2. Methods

2.1. *Least-squares formulation*

A generalized inhomogeneous transformation can be written in the form of a Taylor series expansion about the origin of coordinates where subscript k refers to the Cartesian components of the $\mathbf{z}_L$ coordinate set and subscripts i, j, l refer to Cartesian components of the $\mathbf{x}_L$ coordinate set and L is the particular atom.

$$z_{Lk} = C_k + D_{ki} x_{Li} + \tfrac{1}{2} E_{kij} x_{Li} x_{Lj} + \tfrac{1}{6} F_{kijl} x_{Li} x_{Lj} x_{Ll} + \ldots . \qquad (7)$$

The centroids of each structure should be moved to the origin for the best conditioning of the least-squares method for this problem (Diamond, 1976). The Taylor series will therefore be an expansion about the centroids of the structures. Extending the series to quadratic and cubic derivative terms is analogous to fitting higher polynomial terms in a one-dimensional curve fit. The matrices C, D, E and F are three-dimensional Cartesian tensors of rank 1, 2, 3 and 4 with 3, 9, 18 and 30 independent elements respectively. Symmetry in the derivative tensors E and F reduces the number of independent elements from 27 to 18 and 81 to 30 respectively.

For discrete distributions of atoms, the derivatives in (6) are approximated by finite differences and are best determined by a linear least-squares fit to all the available relatable position vectors. Expanding (7) and collecting like terms for the tensors E and F we obtain

$$\begin{aligned} z_{Lk} = {} & C_k + D_{k1}(x_{L1}) + D_{k2}(x_{L2}) + D_{k3}(x_{L3}) \\ & + E_{k11}(\tfrac{1}{2}x_{L1}^2) + E_{k22}(\tfrac{1}{2}x_{L2}^2) + E_{k33}(\tfrac{1}{2}x_{L3}^2) \\ & + E_{k12}(x_{L1}x_{L2}) + E_{k13}(x_{L1}x_{L3}) \\ & + E_{k23}(x_{L2}x_{L3}) + F_{k111}(\tfrac{1}{6}x_{L1}^3) \\ & + F_{k222}(\tfrac{1}{6}x_{L2}^3) + F_{k333}(\tfrac{1}{6}x_{L3}^3) \\ & + F_{k112}(\tfrac{1}{2}x_{L1}^2 x_{L2}) + F_{k113}(\tfrac{1}{2}x_{L1}^2 x_{L3}) \\ & + F_{k221}(\tfrac{1}{2}x_{L2}^2 x_{L1}) + F_{k223}(\tfrac{1}{2}x_{L2}^2 x_{L3}) \\ & + F_{k331}(\tfrac{1}{2}x_{L3}^2 x_{L1}) + F_{k332}(\tfrac{1}{2}x_{L3}^2 x_{L2}) \\ & + F_{k123}(x_{L1}x_{L2}x_{L3}). \end{aligned} \qquad (8)$$

This can be written compactly as

$$z_{Lk} = \sum_{\mu} A_{k\mu} \xi_{L\mu} \qquad (9)$$

where the unknown tensor elements $A_{k\mu}$ are linearly independent and the constant coefficients $\xi_{L\mu} = \xi_\mu(\mathbf{x}_L)$ are functions of the object coordinates; again subscript k refers to the Cartesian components of the $\mathbf{z}_L$ coordinate set. For quadratic transforms subscript μ takes values from 1 to 10 and, for cubic transforms, values from 1 to 20. The function minimized is the sum of the squared distances between corresponding atoms,

$$\varepsilon = \sum_L \sum_k^3 \left(z_{Lk} - \sum_{\mu} A_{k\mu} \xi_{L\mu} \right)^2 . \qquad (10)$$

The least-squares matrix of second derivatives of ε (Hessian) can be arranged as a block diagonal matrix if the k components of the $\mathbf{z}_L$ coordinate set are separated. These sub-blocks are identical as shown by (11), where δ_{mn} is the Kronecker delta function:

$$\partial^2 \varepsilon / \partial A_{m\psi} \partial A_{n\varphi} = 2\delta_{mn} \sum_L \xi_{L\psi} \xi_{L\varphi}. \qquad (11)$$

Thus the solution for $A_{k\mu}$ can be carried out using separate applications of the least-squares method for each Cartesian index k [of course only one matrix inversion of the sub-block matrix in (11) is required]. A consequence of this is that the superposition of atoms is accomplished by independently matching the projections of the atoms on each Cartesian axis. If the distribution of atoms in space is not uniform (most molecules are anisotropic in shape so this will be the case) then the merit of the fit will be different for each axial projection. The absence of correlation between the superposition of these axial projections can lead to severe or unreasonable distortion of the transformed structure.

2.2. *Geometric restraints*

To prevent unrealistic distortions to the hybridization geometry of the atoms, correlations between the

Cartesian axial projections are introduced by imposing geometric restraints on the object structure. The bond lengths and bond angles are restrained to be within a certain tolerance before and after the transformation. This can be accomplished by adding penalty functions L_{IJ} and L_{IJK} to the residual in (10). L_{IJ} is the bond penalty term between atoms I and J where d_{IJ} is the distance before and d^* the distance after transformation

$$L_{IJ} = \lambda K_{IJ}(d^*_{IJ} - d_{IJ})^2 \tag{12}$$

$$d_{IJ} = [(\mathbf{x}_I - \mathbf{x}_J)(\mathbf{x}_I - \mathbf{x}_J)]^{1/2}$$

$$d^*_{IJ} = \left\{ \sum_k^3 [D_{ki}(x_{Ii} - x_{Ji}) + \tfrac{1}{2}E_{kij}(x_{Ii}x_{Ij} - x_{Ji}x_{Jj}) + \tfrac{1}{6}F_{kijl}(x_{Ii}x_{Ij}x_{Il} - x_{Ji}x_{Jj}x_{Jl})]^2 \right\}^{1/2}$$

$$= \left[\sum_k^3 \left(\sum_{\mu=2} A_{k\mu}\chi_{IJ\mu} \right)^2 \right]^{1/2}, \tag{13}$$

where the coefficients of the tensor elements $\chi_{IJ\mu} = \xi_{I\mu} - \xi_{J\mu}$ are now functions of $\mathbf{x}_I$ and $\mathbf{x}_J$. Similarly for L_{IJK}, θ_{IJK} is the angle between atoms I, J and K before and θ^* the angle after transformation.

$$L_{IJK} = \lambda K_{IJK}(\theta^*_{IJK} - \theta_{IJK})^2 \tag{14}$$

$$\theta_{IJK} = \cos^{-1}\left[\frac{(\mathbf{x}_I - \mathbf{x}_J) \cdot (\mathbf{x}_K - \mathbf{x}_J)}{|\mathbf{x}_I - \mathbf{x}_J||\mathbf{x}_K - \mathbf{x}_J|} \right]$$

$$\theta^*_{IJK} = \cos^{-1}\left\{ \frac{1}{d^*_{IJ}\, d^*_{KJ}} \sum_k^3 \left[\left(\sum_{\mu=2} A_{k\mu}\chi_{IJ\mu} \right) \times \left(\sum_{\mu=2} A_{k\mu}\chi_{KJ\mu} \right) \right] \right\}. \tag{15}$$

The constants K_{IJ} and K_{IJK} are used as relative weighting factors between the restraints. The forms of the penalty functions are similar to common empirical formulations of the steric energy for bonds and bond angles (Weiner, Kollman, Nguyen & Case, 1986). This means that molecular mechanics force constants can be used to scale each restraint and also allow the penalty functions to be interpreted in terms of steric energy. This is done by setting d_{IJ} and θ_{IJK} to their appropriate equilibrium values (depending upon the molecular mechanics force field used) rather than taking on the value before the transformation. The constant λ is used to scale the penalty terms, be they in terms of displacement or steric energy, to the residual function of the tensor elements.

The tensor elements $A_{k\mu}$ now have to be solved for by iterative means; starting with the unrestrained solution any full-matrix quadratic optimizer can be used (for instance a Newton–Raphson that has been modified to ensure global convergence). The first and second derivatives of L_{IJ} and L_{IJK} with respect to $A_{k\mu}$ are given in the Appendix; these are incorporated into the gradient and Hessian [(11)] of the least-squares function, thus providing correlation between Cartesian projections.

Some molecular structures are easily changed into other conformations and in these cases severely weighted penalty terms can easily overperturb the system. So λ should be adjusted carefully to obtain an acceptable difference between original and transformed bond lengths and bond angles or change in steric energy for distortion of the atomic hybridization.

2.3. *Structural extensions*

When implementing the above equations, a few practical problems arise. As with fitting higher- and higher-order polynomials to a data curve, one has to know when to stop adding terms. The variances of the fitted parameters are given by the diagonal elements of the inverse least-squares matrix or Hessian; these should be monitored to determine the merit of the fit. One way to reduce the estimated error in parameters is to increase the data-to-parameter ratio. For a cubic transformation at least 20 atoms are needed to determine all the tensor elements; this will restrict its use to very large structures. However, by supplying extra position vectors the data-to-parameter ratio is increased. This is most easily done by constructing corresponding fractional positions along selected or all bond vectors.

$$\mathbf{x}' = \mathbf{x}_J + [L/(N+1)](\mathbf{x}_I - \mathbf{x}_J) \quad \text{for } L = 1 \text{ to } N. \tag{16}$$

Admittedly this simple data extension will expecially bias the fit for structures that are relatively planar. To circumvent this, atoms involved in π bonding have additional points positioned above and below the plane that are perpendicular to the presumed trigonally connected atoms. The new position vectors are constructed as follows:

$$\mathbf{x}' = \mathbf{x}_I \pm P_I[(\mathbf{x}_J - \mathbf{x}_M) \wedge (\mathbf{x}_K - \mathbf{x}_M)]/|(\mathbf{x}_J - \mathbf{x}_M) \wedge (\mathbf{x}_K - \mathbf{x}_M)|, \tag{17}$$

where atoms J, K and M are attached to atom I with sp^2 hybridization. The scaling parameter P_I serves to adjust the length of the attached vector. Other more complicated methods can be envisaged, for instance matching points on the van der Waals surfaces of each structure.

2.4. *Robust analysis*

The least-squares criterion for an optimal fit is very sensitive to outlying points. If there are a few atoms that are obviously not going to superimpose they can be removed from the analysis, or a more robust analysis can be performed. Robust means that the fitted parameters will be less sensitive to outlying data

Table 1. *Orthogonal (O), linear (L), quadratic (Q) and cubic (C) transformation fitting parameters for deforming the ketone over the lactone*

The starred transformations deform the lactone over the ketone. The r.m.s. deviations are measured in ångströms and degrees. Ratio refers to the data-to-parameter ratio. N is the number of extra points between bonds, and P_I is the distance in ångströms of the extra points above and below the plane for the π-bonded atoms. λ_B and λ_A are the scaling factors for the bond-length and bond-angle penalty terms; if a value was not specified then restraints were not included.

	R.m.s. atom–atom distance	Ratio (N, P_I)	R.m.s. bond difference (λ_B)	R.m.s. angle difference (λ_A)	Remarks
O1	0·660	11·50			From *L1*
O2	0·505	11·50			Optimal
O3	0·548	11·50			Robust
O4	0·824	11·50			Inverted
L1	0·314	5·75	0·1918	21·32	
L2	0·355	5·75	0·2281	20·92	Robust
L3	0·459	5·75	0·0311 (10)	1·52	Restrained
L4	0·438	10·25 (0, 1·0)	0·0663	3·59	
Q1	0·119	2·30	0·0839	4·72	
Q2	0·125	9·50 (3)	0·0825	5·25	
Q3	0·139	9·50 (3)	0·0664	3·73	Robust
Q4	0·165	11·30 (3, 1·0)	0.0818	4·44	
Q5	0·177	9·50 (3)	0·0254 (10)	1·47 (10)	Restrained
Q6	0·260	9·50 (3)	0·0118 (100)	0·76 (100)	Restrained
Q7	0·131	110·30 (45)	0·0838	5·73	
Q8	0·284	11·30 (3, 1·5)	0·0137 (100)	0·79 (100)	Restrained
C1	0·010	1·15	0·0885	2·73	
C2	0·024	10·75 (8)	0·0855	2·53	
C3	0·043	10·75 (8)	0·0749	2·91	Robust
C4	0·093	11·65 (8, 1·5)	0·0929	3·80	
C5	0·088	10·75 (8)	0·0185 (10)	1·03 (10)	Restrained
C6	0·143	10·75 (8)	0·0058 (100)	0·55 (100)	Restrained
C7	0·027	55·15 (45)	0·0861	2·54	
C8	0·179	11·65 (8, 1·5)	0·0129 (100)	0·70 (100)	Restrained
*L1**	0·474	7·67	0·0740	6·95	
*Q2**	0·155	9·50 (3)	0·0923	2·79	Inverted
*Q4**	0·179	11·30 (3, 1·0)	0·0507	2·65	
*Q5**	0·181	9·50 (3)	0·0291 (10)	1·09 (10)	Inverted
*C2**	0·068	10·75 (8)	0·0801	2·60	Inverted
*C4**	0·115	11·65 (8, 1·5)	0·0613	2·92	
*C5**	0·108	10·75 (8)	0·0172 (10)	0·90 (10)	Inverted

points (atoms). One method is to minimize the absolute deviation

$$\varepsilon = \sum_L \left| z_{Lk} - \sum_\mu A_{k\mu} \xi_{L\mu} \right|. \qquad (18)$$

Each Cartesian projection k is minimized separately. The optimization is most easily accomplished using a simplex algorithm (Shavers, Parsons & Deming, 1979) which has no difficulties with discontinuities in the residual error surface. The simplex is conveniently initiated from the least-squares solution by randomly perturbing the value of the tensor elements by some fraction of their variances.

3. Discussion

The various transformations are demonstrated using two structures with similar atomic skeletons; a five-membered ring lactone and a cyclopentanone both with an adjoining benzylidene group (Kearsley & Desiraju, 1985). The comparison parameters are shown in Table 1 and the orthogonal transformation *O2* depicted in Fig. 2 shows the original conformation of each molecule. On the ketone, the hydrogen atoms on the carbon that correspond to the lactone oxygen have been removed for the comparison. The conformation of the lactone is almost planar; only the

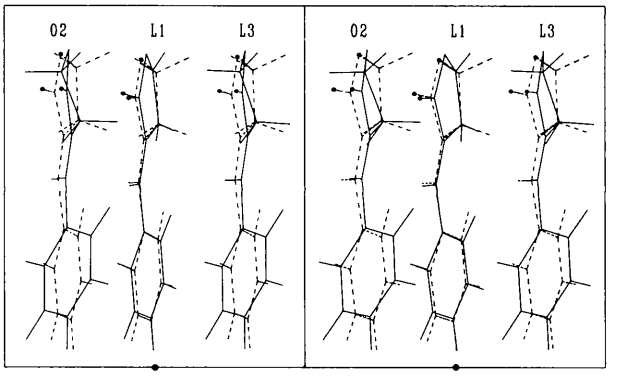

Fig. 2. Stereo drawing of the superposition comparison of the optimal orthogonal (*O2*), linear (*L1*) and geometrically restrained linear (*L3*) transformations. The planar lactone is drawn with dashed lines. The ketone, which undergoes the transformations, is drawn with solid lines.

methylene hydrogens are substantially offset from the least-squares plane. In comparison, the cyclopentanone is puckered and the five- and six-membered rings are not in the same plane. The lactone is treated as the reference structure and the ketone undergoes the transformations in an attempt to remove the twists about the connecting bonds between the rings. All the individual weighting factors, K_{IJ} and K_{IJK}, are set to unity.

The optimal orthogonal transformation $O2$ clearly shows that the structures are different (see Fig. 2). Note that the rotation matrix factorized from the homogeneous distortion tensor gives an inferior superposition; compare $O1$ and $O2$ in Table 1. Orthogonal transformation $O4$ compares the ketone to the crystallographically inverted lactone. The match is far worse since corresponding methylene hydrogens are now on opposite sides of the five-membered ring. All the other transformations correct for this by inverting the ketone with an improper rotation.

The r.m.s. deviation of distance for the linear transformation $L1$ shows a marked improvement over the orthogonal transformations. However, this is deceptive since scrutiny of Fig. 2 will show that most of the atoms have been crushed down onto the best plane of the lactone; the smallest eigenvalue of T is indicative of this (0·3295, 0·9737, 1·0476). The geometry of the cyclopentanone group is therefore severely distorted. $L3$ in Fig. 2 shows how the bond-length restraints re-establish the near-original ketone conformation. It is interesting to note that the abrupt drop in the r.m.s. difference in angle between $L2$ and $L3$ is due purely to the bond restraints. Also, as the bond penalty terms for the linear transformation become overriding (λ_B tends to infinity) the limiting r.m.s. deviation of distance is that of the orthogonal transformation $O2$. In comparison, restricting the bond angles to their precise values gives a limiting r.m.s. deviation of distance of 0·502 Å.

$Q2$ in Fig. 3 shows that the quadratic transformation removes the torsional twists between the rings but cannot avoid deforming the hydrogens from the plane of the benzene ring. Even after the application of geometric restraints ($Q6$), which re-establishes the correct puckering of the cyclopentanone ring, the benzene ring remains distorted. Also, the torsions reappear between the rings.

The cubic transform ($C2$) almost precisely superimposes the molecules. Geometric restraints ($C6$, Fig. 3) seem to push the wrong carbon out of plane (the carbon corresponding to the lactone oxygen). This is explicable since it is preferable to fit three atoms of the adjacent methylene group rather than a single carbon; the geometric restrictions can be satisfied either way (alternative weighting schemes or the addition of restraints that enforce planarity would remedy this problem). Nevertheless the cubic transformation suggests that the difference between the structures is localized at the puckering of the cyclopentanone ring and all other distortions uniformly embrace the whole structure.

Examination of Table 1 shows that the r.m.s. deviation of distance increases slightly as the number of points between bonds [N in (16)] increases. The value of N was set when the data-to-parameter ratio reached 10 or the variances of the tensor elements stabilized. There are nine sp^2 carbons in common between the structures and therefore 18 additional position vectors could be constructed according to (17). This substantially decreased the variances of the tensor elements and prevented the tendency of the ketone to contract along the largest inertial axis.

The robust fits ignored matching the methylene hydrogen in favour of a better fit to the carbon skeleton. They were far inferior to the restrained fits. Robust analyses would fare better when there are no pathological dilations and only a few of the atoms are severely outlying.

Alternatively, the lactone can be deformed over the ketone structure. This will not in general give the same comparison; only the optimal orthogonal transformation gives the same superposition. Linear transformations give a far worse r.m.s. deviation of distance (compare $L1$ and $L1^*$ in Table 1), because although the linear transform can suppress curvature and out-of-plane deviations in the ketone it cannot introduce the required twists in the lactone. Also, in this example, the quadratic and cubic transformations on the lactone are problematical since it appears that the structure is inverted according to the factorization of the D tensor. For $Q2^*$ the eigenvalues of T are (0·6973, 1·0071, 1·7082). These immense homogeneous dilations are compensated for by inhomogeneous distortions which wrench the hydrogens back onto the correct side of the five-membered ring. Application of geometric restraints could not remove the

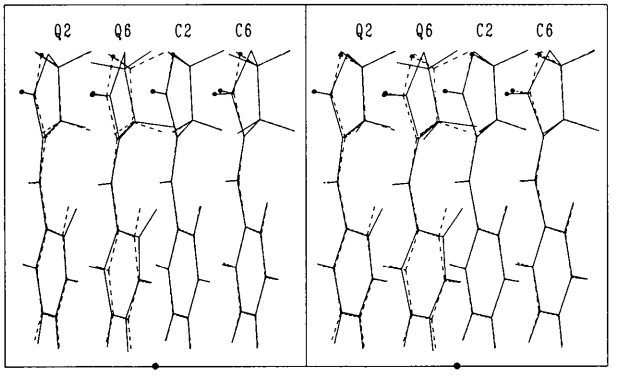

Fig. 3. Stereo drawing of the superposition comparison of quadratic transformation, free and restrained ($Q2$ and $Q6$), and cubic transformation, free and restrained ($C2$ and $C6$). The planar lactone is drawn with dashed lines. The ketone, which undergoes the transformations, is drawn with solid lines.

improper rotation or decrease the variance in the tensor parameters which were very large. The awkwardness of these inhomogeneous transformations vanishes if extra position vectors are constructed above and below the plane of the π-bonded atoms according to (17). For instance, for $Q4^*$ the variances of the tensor parameters are an order of magnitude smaller and the eigenvalues of T indicate only minor amounts of homogeneous dilation (0·9601, 0·9770, 1·0123).

When examining the above transformations it becomes clear that to characterize low-order inhomogeneous transformations successfully requires that data (atoms) be distributed evenly through space for both reference and object structures. For most structural comparisons one does not expect to see large homogeneous dilations or severe changes in curvature. This suggests that the tensor parameters themselves can be directly constrained to have small values or values that will reflect only small changes in strain (variation of T) but allow for twists and bends. Unfortunately variations in R and T are not easily separable for inhomogeneous transformations and the construction of penalty functions that would not bias the comparisons would be difficult.

What sort of deformations are characteristic of a cubic transform? Diamond (1976) has shown that quadratic transforms can bend and twist the structure in arcs of constant curvature; in the above example we see that this is not sufficient to iron out the ketone if the atomic hybridization is to remain reasonable. Fig. 4 shows two methods of viewing the displacement field (related to the strain field) that transforms chair cyclohexane into its planar conformation. The conformations were first superimposed using an orthogonal transformation to eliminate the pure rotation displacements. The subsequent cubic transformation shows no quadratic contribution and only a minor amount of homogeneous strain. It can be seen that the cubic terms serve to unpucker the cyclohexane ring. In general a cubic transformation will accommodate structures where the variation in bending and twisting (curvature) is skewed with respect to the centroid.

The distortion tensors that were obtained from a particular structural comparison apply continuously over the region they were characterized from. Extrapolation outside the region of fit is possible but will most likely lead to calamitous results. As was alluded to in the *Introduction*, it would not be difficult to develop model distortion fields that could be used to perturb or modify structures. A simple prescription for applying a continuous twist would be to match a regular cubic grid of points to one that had each plane of points rotated relative to the adjacent plane by a constant angle about the twist axis. Next, apply the comparison procedure to the original and distorted grids to derive the transformation tensors. To apply the twisting distortion, one has only to centre and align a structure in the distortion field prior to the coordinate transformation. For instance, if the coordinates of an amino-acid residue were excised from a helical protein substructure and the pieces joined, subsequent optimization of this severe local distortion will probably tear adjacent residues away from the ideal helical form. However, this rending of the helical chain can be prevented by slightly twisting and stretching the chain fragments so that the new bond is more or less at the correct distance; thus, once joined, the entire substructure is only marginally distorted.

In conclusion we note that the preferred method of interpretation or appreciation of such structural comparisons still relies heavily on qualitative visual identification of similar regions, yet this is enhanced dramatically if the low-order global distortions are removed between the structures. Furthermore, the methods presented here are not intended to provide alternative standard measures of structural similarity but rather as a recourse to a better structural analysis. More sophisticated restraints such as selected proper and improper torsion-angle restrictions will help

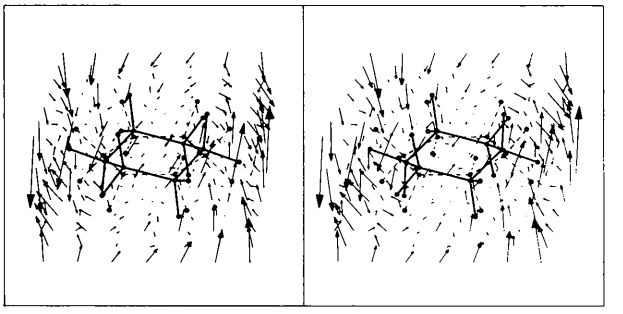

(*a*)

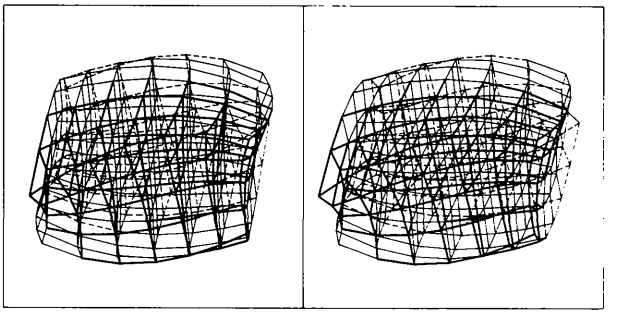

(*b*)

Fig. 4. Stereo diagrams depicting the cubic deformation that forces chair cyclohexane into its planar conformation. (*a*) shows how the displacement vectors move the methylene groups alternatively up and down around the ring. (*b*) shows how a rectangular block of cubes distorts under the same cubic transformation. In both representations, the cubic tensor elements have been scaled down by 1/5 for clarity.

maintain atoms in the same plane where needed – indeed, a full molecular mechanics force field could be installed to monitor the total steric energy.

I would like to thank Dr J. M. McBride for his advice in general and criticism of this paper. I would also like to acknowledge Dr J. H. Prestegard for procuring for SKK the Anderson Fellowship in 1987. This work was carried out at the Department of Chemistry, Yale University, New Haven, CT 06511, USA, and supported by the US Office of Naval Research (Contract N00014087-K-0437).

APPENDIX

Equations (19) and (20) give the first and second derivatives of L_{IJ} with respect to $A_{k\mu}$:

$$\frac{\partial L_{IJ}}{\partial A_{n\varphi}} = 2\lambda K_{IJ}\frac{[d^*_{IJ}-d_{IJ}]}{d^*_{IJ}}\left(\sum_{\mu=2} A_{n\mu}\chi_{IJ\mu}\right)\chi_{IJ\varphi} \quad (19)$$

$$\frac{\partial^2 L_{IJ}}{\partial A_{m\psi}\,\partial A_{n\varphi}}$$

$$= \frac{2\lambda K_{IJ}}{d^*_{IJ}}\left[\frac{d_{IJ}}{d^{*2}_{IJ}}\left(\sum_{\mu=2} A_{m\mu}\chi_{IJ\mu}\right)\left(\sum_{\mu=2} A_{n\mu}\chi_{IJ\mu}\right) + [d^*_{IJ}-d_{IJ}]\delta_{nm}\right]\chi_{IJ\psi}\chi_{IJ\varphi}. \quad (20)$$

The derivatives of L_{IJK} with respect to $A_{k\mu}$ are realized by the applications of the chain rule. Let $U = \cos\theta^*_{IJK} = X/(YZ)^{1/2}$; then the first and second derivatives of L_{IJK} are given by (21)–(22) and derivatives with respect to U by (23)–(24).

$$\frac{\partial L_{IJK}}{\partial A_{n\varphi}} = \frac{2\lambda K_{IJK}}{\sin\theta^*_{IJK}}(\theta_{IJK}-\theta^*_{IJK})\frac{\partial U}{\partial A_{n\varphi}} \quad (21)$$

$$\frac{\partial^2 L_{IJK}}{\partial A_{m\psi}\,\partial A_{n\varphi}}$$

$$= \frac{2\lambda K_{IJK}}{\sin\theta^*_{IJK}}\left[(\theta_{IJK}-\theta^*_{IJK})\frac{\partial^2 U}{\partial A_{m\psi}A_{n\varphi}} + \frac{1+(\theta_{IJK}-\theta^*_{IJK})\cot\theta^*_{IJK}}{\sin\theta^*_{IJK}}\frac{\partial U}{\partial A_{m\psi}}\frac{\partial U}{\partial A_{n\psi}}\right] \quad (22)$$

$$\frac{\partial U}{\partial A_{n\varphi}} = (YZ)^{-1/2}\frac{\partial X}{\partial A_{n\varphi}} - \frac{U}{2}\left(\frac{1}{Y}\frac{\partial Y}{\partial A_{n\varphi}} + \frac{1}{Z}\frac{\partial Z}{\partial A_{n\varphi}}\right) \quad (23)$$

$$\frac{\partial^2 U}{\partial A_{m\psi}\,\partial A_{n\varphi}} = (YZ)^{-1/2}\left[\frac{\partial^2 X}{\partial A_{m\psi}A_{n\varphi}} - \frac{1}{2}\left(\frac{1}{Y}\frac{\partial Y}{\partial A_{m\psi}} + \frac{1}{Z}\frac{\partial Z}{\partial A_{m\psi}}\right)\frac{\partial X}{\partial A_{n\varphi}}\right] - \frac{1}{2}\frac{\partial U}{\partial A_{m\psi}}\left(\frac{1}{Y}\frac{\partial Y}{\partial A_{n\varphi}} + \frac{1}{Z}\frac{\partial Z}{\partial A_{n\varphi}}\right) + \frac{U}{2}\left(\frac{1}{Y^2}\frac{\partial Y}{\partial A_{m\psi}}\frac{\partial Y}{\partial A_{n\varphi}} + \frac{1}{Z^2}\frac{\partial Z}{\partial A_{m\psi}}\frac{\partial Z}{\partial A_{n\varphi}} - \frac{1}{Y}\frac{\partial^2 Y}{\partial A_{m\psi}A_{n\varphi}} - \frac{1}{Z}\frac{\partial^2 Z}{\partial A_{m\psi}A_{n\varphi}}\right). \quad (24)$$

The first and second derivatives of X and Y are given by (25)–(28) and the derivatives of Z as for Y with IJ replaced by JK.

$$\frac{\partial X}{\partial A_{n\varphi}} = \left(\sum_{\mu=2} A_{n\mu}\chi_{IJ\mu}\right)\chi_{JK\varphi} + \left(\sum_{\mu=2} A_{n\mu}\chi_{JK\mu}\right)\chi_{IJ\varphi} \quad (25)$$

$$\frac{\partial^2 X}{\partial A_{m\psi}\,\partial A_{n\varphi}} = (\chi_{IJ\psi}\chi_{JK\varphi} + \chi_{JK\psi}\chi_{IJ\varphi})\delta_{mn} \quad (26)$$

$$\frac{\partial Y}{\partial A_{n\varphi}} = 2\left(\sum_{\mu=2} A_{n\mu}\chi_{IJ\mu}\right)\chi_{IJ\varphi} \quad (27)$$

$$\frac{\partial^2 Y}{\partial A_{m\psi}A_{n\varphi}} = 2\chi_{IJ\psi}\chi_{IJ\varphi}\delta_{mn}. \quad (28)$$

References

COX, J. M. (1967). *J. Mol. Biol.* **28**, 151–156.
DIAMOND, R. (1966). *Acta Cryst.* **21**, 253–266.
DIAMOND, R. (1976). *Acta Cryst.* A**32**, 1–10.
KABSCH, W. (1976). *Acta Cryst.* A**32**, 922–923.
KABSCH, W. (1978). *Acta Cryst.* A**34**, 827–828.
KEARSLEY, S. K. (1989). *Acta Cryst.* A**45**, 208–210.
KEARSLEY, S. K. & DESIRAJU, G. R. (1985). *Proc. R. Soc. London Ser. A*, **397**, 157–181.
KENKNIGHT, C. E. (1984). *Acta Cryst.* A**40**, 709–712.
LESK, A. M. (1986). *Acta Cryst.* A**42**, 110–113.
MACKAY, A. L. (1977). *Acta Cryst.* A**33**, 212–215.
MACKAY, A. L. (1984). *Acta Cryst.* A**40**, 165–166.
MCLACHLAN, A. D. (1972). *Acta Cryst.* A**28**, 656–657.
MCLACHLAN, A. D. (1979). *J. Mol. Biol.* **128**, 49–79.
NYBURG, S. C. (1974). *Acta Cryst.* B**30**, 251–253.
RAO, S. T. & ROSSMAN, M. G. (1973). *J. Mol. Biol.* **76**, 241–256.
SHAVERS, C. L., PARSONS, M. L. & DEMING, S. N. (1979). *J. Chem. Educ.* **56**, 307–309.
WATKIN, D. J. (1980). *Acta Cryst.* A**36**, 975–978.
WEINER, S. J., KOLLMAN, P. A., NGUYEN, D. T. & CASE, D. A. (1986). *J. Comput. Chem.* **7**, 230–252.